available at www.sciencedirect.com

ScienceDirect

journal homepage: www.ejconline.com

The UGT1A1*28 polymorphism correlates with erlotinib's effect on SN-38 glucuronidation

Yong Liu [a], *Jacqueline Ramírez* [a], *Larry House* [a], *Mark J. Ratain* [a,b,c,*]

[a] *Department of Medicine, The University of Chicago, Chicago, IL 60637, USA*
[b] *Committee on Clinical Pharmacology and Pharmacogenomics, The University of Chicago, Chicago, IL 60637, USA*
[c] *Cancer Research Center, The University of Chicago, Chicago, IL 60637, USA*

ARTICLE INFO

Article history:
Received 5 February 2010
Received in revised form 21 April 2010
Accepted 23 April 2010
Available online 23 May 2010

Keywords:
Erlotinib
Irinotecan
SN-38 glucuronidation
UGT1A1*28
Drug–drug interactions

ABSTRACT

The combination of irinotecan and erlotinib has been evaluated in clinical trials, although toxicity has been significant. We aimed to investigate the effect of erlotinib on SN-38 glucuronidation and the association between UGT1A polymorphisms and SN-38 glucuronidation activity in the presence of erlotinib. The inhibitory effect of erlotinib on SN-38 glucuronidation was determined by measuring the formation rates for SN-38 glucuronide, using recombinant human UGT1A1, pooled human liver microsomes (HLMs) and 52 Caucasian liver microsomes in the absence or presence of erlotinib. Inhibition kinetic studies were conducted. AUC ratios were used to predict the risk of potential drug–drug interactions (DDI) *in vivo*. Our data showed that erlotinib exhibited potent non-competitive inhibition against SN-38 glucuronidation in pooled HLMs and UGT1A1. Using the physiological and pharmacokinetic parameters obtained from the literature, we estimated the *in vivo* concentrations of unbound erlotinib available for UGT1A1 active site and thus the AUC ratios of SN-38 were also quantitatively predicted. It is estimated that erlotinib administered at 50 mg/day or higher doses may result in at least a 24% increase in SN-38 AUC. Significant correlations were observed between SN-38 glucuronidation activity in the presence of erlotinib and UGT1A1*28 in 52 Caucasian liver microsomes. Our results suggest that erlotinib is a potent inhibitor of SN-38 glucuronidation via UGT1A1 inhibition. The coadministration of erlotinib with irinotecan may result in clinically significant DDI. UGT1A1*28 polymorphism correlates with erlotinib's effect on SN-38 glucuronidation. The present findings shed light on the development and optimisation of combinations involving irinotecan and erlotinib.

1. Introduction

Irinotecan is one of the most commonly prescribed chemotherapy agents. Despite the extensive clinical experience with irinotecan, its usage has been limited by severe toxicity, including diarrhoea and neutropaenia. Fatal events (up to 5.3%) during single-agent irinotecan treatment have been reported.[1] The risk of life-threatening neutropaenia of irinotecan has been consistently associated with genetic variation in UGT1A1.[2,3] Irinotecan requires metabolic activation by carboxylesterase 2 to form the active metabolite SN-38, which is further cleared via formation of SN-38 glucuronide (SN-38G) by UGT1A isoforms in human liver, including UGT1A1, 1A3, 1A6 and 1A9. Among these UGT isoforms, UGT1A1 shows

* *Corresponding author:* Address: The University of Chicago, 5841 South Maryland Avenue, MC 2115, Chicago, IL 60637, USA. Tel.: +1 773 7024400; fax: +1 773 7023969.
E-mail address: mratain@medicine.bsd.uchicago.edu (M.J. Ratain).
0959-8049/$ - see front matter © 2010 Elsevier Ltd. All rights reserved.
doi:10.1016/j.ejca.2010.04.022

the highest activity of SN-38 glucuronidation.[4] There is accumulating evidence that plasma exposure to SN-38 is associated with increased risk of severe toxicity, primarily diarrhoea and neutropaenia.[2,5] The UGT1A1*28 polymorphism has been shown to be associated with reduced glucuronidation of SN-38,[6,7] and increased clinical toxicity for patients treated with irinotecan.[2,8] We have showed that erlotinib is a potent inhibitor of UGT1A1-mediated 4-methylumbelliferone glucuronidation and bilirubin glucuronidation.[9] These findings prompted us to assume that drug–drug interactions (DDIs) might occur between erlotinib and irinotecan via the inhibition of UGT1A1-mediated SN-38 glucuronidation and that genetic variation in UGT1A1 gene might be associated with the toxical outcome of the combination of both drugs.

Anti-epidermal growth factor receptor (EGFR) therapies have been utilized in combination with chemotherapy in multiple solid tumours, including colorectal and lung cancers.[10] Targeting the EGFR pathway using a monoclonal antibody, such as cetuximab, has been demonstrated to be safe and effective when given alone or in combination with irinotecan.[11]

Recently, the combination of irinotecan and erlotinib, an orally available, potent and selective EGFR small molecule inhibitor approved for treatment of non-small cell lung and pancreatic cancer,[12] has been evaluated in some studies. However, contradictory results have been reported with respect to the safety of the combination of irinotecan and erlotinib. It has been shown that erlotinib can enhance the antitumour activity of irinotecan, without enhanced toxicity, in the LoVo human colorectal tumour xenograft model.[13] A clinical study of erlotinib with capecitabine and irinotecan in advanced colorectal cancer patients indicated that the combination has an acceptable safety profile and appears suitable for further phase II studies.[14] However, a phase I trial of irinotecan, infusional 5-fluorouracil and leucovorin (FOLFIRI) with erlotinib was halted due to unexpectedly severe toxicities in several patients, including rash, diarrhoea and neutropaenia, even at the lowest dose level.[15]

In this study, we found that erlotinib exhibited a potent non-competitive inhibition against SN-38 glucuronidation in pooled human liver microsomes (HLMs) and recombinant UGT1A1. The potential for drug interactions between erlotinib and SN-38 was estimated using the area under the plasma concentration–time curve (AUC) ratios. Significant correlations were observed between UGT1A1*28 and SN-38G formation rates in the absence and presence of erlotinib in 52 Caucasian liver microsomes.

2. Materials and methods

2.1. Chemicals

Erlotinib was purchased from Biaffin GmbH & Co KG (Kassel, Germany). SN-38 was obtained from Toronto Research Chemicals, Inc. (North York, Canada), SN-38G was gift kindly provided by Dr. Kiyoshi Terada (Yakult Honsha Co. Ltd., Japan). β-Glucuronidase (from *Escherichia coli*), alamethicin (from *Trichoderma viride*), Tris–HCl, ketoconazole and UDPGA (trisodium salt) were purchased from Sigma–Aldrich (St. Louis, MO, USA). All other reagents were of HPLC grade or of the highest grade commercially available.

2.2. HLMs and liver tissue

Pooled HLMs and human UGT1A1 expressed in baculovirus-infected insect cells were purchased from BD Gentest Corp. (Woburn, MA, USA). Pooled HLMs were derived from 22 donors (90% Caucasian, 5% Hispanic and 5% African-American; 15 men and 7 women). The median age was 48 years with a range of 10–70.

Human liver tissue from 52 Caucasian donors was processed through Dr. Mary Relling's Laboratory at St. Jude Children's Research Hospital (Memphis, TN, USA) and was provided by the Liver Tissue Procurement and Distribution System (funded by #NO1-DK-9-2310) and by the Cooperative Human Tissue Network. Samples were collected with human subjects' approval.

2.3. SN-38 glucuronidation assay

Incubations were performed using conditions reported previously[16] with a slight modification. Incubation was performed at 37 °C for 30 min. Microsomes were pre-incubated with 50 μg/mg protein alamethicin on ice for 15 min prior to incubation. SN-38 was dissolved in DMSO. The final concentration of DMSO in the incubation system was 1% (v/v). HPLC separation was achieved using a C18 column (3.9×300 mm I.D., 10 μm) (Sigma–Aldrich, St. Louis, MO) at a flow rate of 1 ml/min and fluorescence detection at λ_{ex} 355 nm and λ_{em} 515 nm. A mobile phase consisted of 32/0.5/67.5 acetonitrile/tetrahydrofuran/5 mM 1-heptanesulphonic acid in 50 mM potassium phosphate buffer (pH 2.7). The metabolites were quantified using the ratio of SN-38G to internal standard calibration curve. The precision was assessed by relative standard deviation (RSD = SD/Mean × 100%), while the accuracy was calculated as relative mean error of calculated concentrations from nominal concentrations [RME = (calculated concentration – nominal concentration)/nominal concentration × 100%]. The accuracy and precision of the back-calculated values for each concentration were less than 15% of the nominal values.

2.4. Kinetic study in pooled HLMs and UGT1A1

SN-38 (1–20 μM) was preincubated with pooled HLMs (0.5 mg/ml) or UGT1A1 (0.25 mg/ml) at 37 °C for 5 min in a final volume of 200 μl of 25 mM Tris–HCl buffer (pH 7.4) containing 10 mM $MgCl_2$ and 50 μg/mg protein alamethicin. After preincubation of the reaction mixture, the reaction was started by adding UDPGA for a final concentration of 5 mM. Incubation was performed at 37 °C for 30 min. All experiments were performed in duplicate.

2.5. Inhibition of SN-38 glucuronidation activity assay

SN-38 was incubated in the presence of different concentrations of erlotinib (0, 0.05, 0.1, 0.2, 0.5, 1, 2, 10 and 50 μM). Ketoconazole, a known inhibitor of SN-38 glucuronidation,[17] was used as a positive control. The reactions were continued for

30 min at 37 °C in 0.5 mg/ml HLMs or 0.25 mg/ml UGT1A1. All experiments were separately performed in duplicate.

2.6. Genotyping and correlation studies in HLMs

Fifty-two Caucasian liver microsomes were incubated with SN-38 with or without erlotinib as described above to determine the correlation of SN-38 glucuronidation activities in the absence or presence of erlotinib with genotypes of UGT1A1. Genotyping of UGT1A1*28 polymorphisms has been previously performed in the entire set of 52 Caucasian liver samples.[18]

2.7. Kinetics analysis

Kinetic constants for SN-38 glucuronidation were obtained by fitting the experimental data to the Michaelis–Menten formula [Eq. (1)],[19]

$$v = (V_{max}S)/(K_m + S) \quad (1)$$

where v is the rate of reaction, V_{max} is the maximum velocity, K_m is Michaelis constant (substrate concentration at half of V_{max} of the reaction) and S is the substrate concentration.

The inhibition constant (K_i) values were determined using a range of concentrations of SN-38 (2–10 μM) and different concentrations of erlotinib (0–2 μM). Inhibition data from experiments were graphically represented by Dixon plots and K_i values were calculated with non-linear regression according to the equations for competitive [Eq. (2)], non-competitive [Eq. (3)],[19]

$$v = (V_{max}S)/(K_m(1 + I/K_i) + S) \quad (2)$$

$$v = (V_{max}S)/(K_m + S)(1 + I/K_i) \quad (3)$$

where I is the inhibitor concentration and K_i is the inhibition constant describing the affinity of the inhibitor for the enzyme. The type of inhibition was determined from the fitting of data to the enzyme inhibition models. Goodness of fit to kinetic and inhibition models was assessed from the F statistic, r^2 values, parameter standard error estimates and 95% confidence intervals. Kinetic constants are reported as the value ± standard error of the parameter estimate. IC_{50} values (concentration of inhibitor that reduces enzyme activity by 50%) were determined by GraphPad Prism4 software (GraphPad Software Inc., La Jolla, CA).

2.8. Predicted concentrations of erlotinib at UGT catalytic sites

In view of the general assumption that only unbound drug is available for interaction with the enzyme active site, and in order to exclude the highest risk, we used the maximum unbound hepatic input concentration ($[I]_{in,u}$) as the inhibitor concentration at UGT active site. The concentration was determined as described previously.[9]

2.9. Calculation of AUC_i/AUC ratio

The magnitude of inhibitory interactions of erlotinib was estimated as the ratio of the area under the plasma concentration–time curve of SN-38 in the presence and absence of erlotinib (AUC_i/AUC). This ratio was determined as we described previously.[9]

2.10. Data analysis and statistics

The t-test analysis was performed to assess the variance in SN-38G formation in the absence or presence of erlotinib in the whole population of 52 HLMs and between different genotypes, and spearman correlation analysis of each genotype versus SN-38G formation was performed by GraphPad Prism4 software (GraphPad Software Inc., La Jolla, CA). The threshold for statistical significance was set at $P < 0.05$. All tests were two-sided.

3. Results

3.1. Kinetic studies in pooled HLMs and recombinant UGT1A

SN-38G formation rates were linear with microsomal protein concentration up to 1 mg/ml and time up to 1 h (data not shown). The kinetics of SN-38 glucuronidation in pooled HLMs (0.5 mg /ml) and recombinant UGT1A1 (0.25 mg/ml) were investigated. SN-38 (1–20 μM) was incubated with pooled HLMs or UGT1A1 at 37 °C for 30 min. The values of apparent K_m in HLMs and UGT1A1 were 4.1 ± 0.3 and 2.5 ± 0.3 μM, respectively. The values of apparent V_{max} in HLMs and UGT1A1 were 256 ± 8 and 2505 ± 103 pmol/min/mg protein, respectively.

3.2. Inhibition of SN-38 glucuronidation activity by erlotinib in pooled HLMs

SN-38 glucuronidation rates in the presence of various concentrations of potential inhibitors were investigated in pooled HLMs. The concentration of substrate, SN-38, was 5 μM, which was close to its K_m value. The IC_{50} value of ketoconazole in HLMs was calculated as 8.0 ± 0.3 μM, which is comparable with the previously published data.[17]

Erlotinib exhibited a UDPGA- and concentration-dependent inhibition against SN-38 glucuronidation activity in HLMs. The IC_{50} value was calculated as 0.58 ± 0.05 μM. No glucuronidation of erlotinib was found in the course of the incubations.

3.3. Inhibition kinetic analysis in pooled HLMs and recombinant UGT1A1

Erlotinib was found to strongly inhibit SN-38G formation in pooled HLMs. The representative Lineweaver–Burk plots (Fig. 1A) and analysis of the parameters of the enzyme inhibition model suggested that the inhibition type was non-competitive. Based on analysis of non-linear regression of inhibition data and Dixon plots presented in Fig. 1B, erlotinib showed non-competitive inhibition against SN-38 glucuronidation in pooled HLMs with a K_i of 0.68 ± 0.04 μM. Erlotinib also exerted non-competitive inhibition against SN-38 glucuronidation in recombinant UGT1A1 with a K_i of 0.81 ± 0.05 μM (Fig. 1C and D).

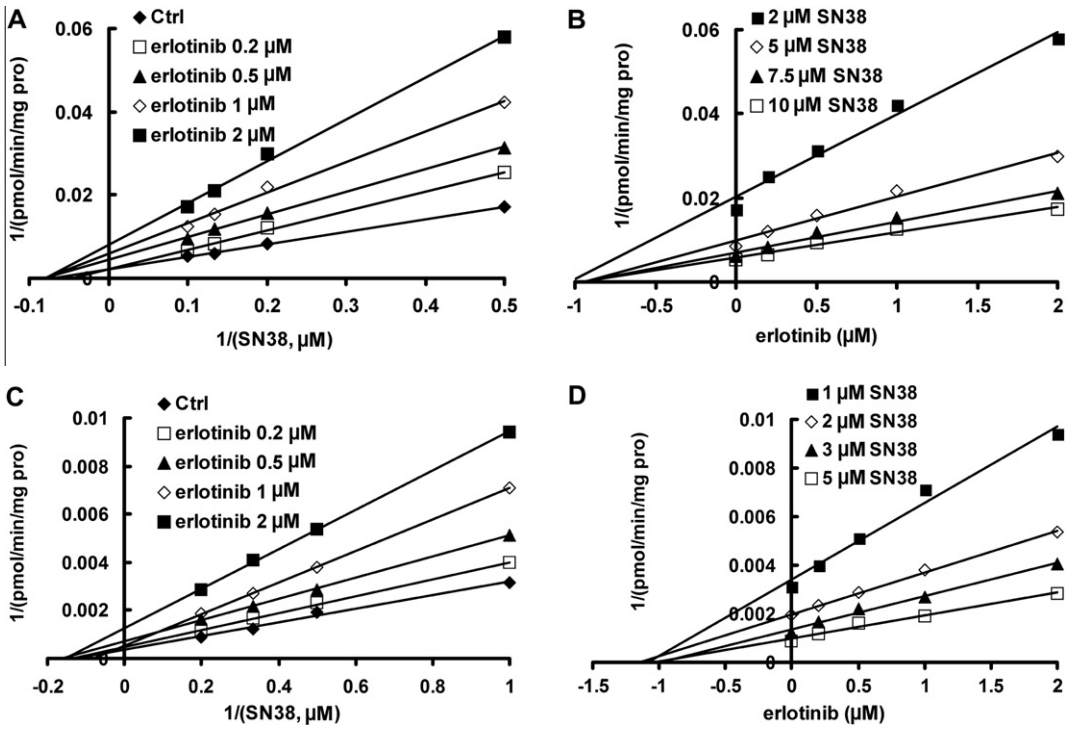

Fig. 1 – Representative Lineweaver–Burk plots (A, C) and Dixon plots (B, D) of the effects of erlotinib on SN-38 glucuronide formation in pooled human liver microsomes (A, B) and recombinant UGT1A1 (C, D). Reactions were performed in the presence of SN-38 and various concentrations of erlotinib (0, 0.2, 0.5, 1 and 2 μM) in pooled human liver microsomes (0.5 mg/ml) or recombinant UGT1A1 (0.25 mg/ml), 50 μg/mg protein alamethicin, 5 mM UDPGA and 10 mM $MgCl_2$ in a 25 mM Tri–HCl buffer (pH 7.4) in a final volume of 200 μl at 37 °C for 30 min. All data points shown represent the mean of duplicate measurements.

3.4. *Calculated AUC ratio of SN-38 in the presence and absence of erlotinib*

The values of $[I]_{max}$ after oral administration of 50, 100 and 150 mg/day erlotinib were calculated as 1.42, 2.64 and 3.72 μM, respectively. The calculated values are comparable to the reported actual values (1.29, 2.53 and 3.65 μM) and fall inside the interval of variability.[20,21] The values of $[I]_{in,u}$ after oral administration of 50, 100 and 150 mg/day erlotinib were calculated as 0.16, 0.18 and 1.46 μM, respectively.

After oral administration of erlotinib of 50, 100 and 150 mg/day, the AUC of coadministered SN-38 is predicted to increase by 24%, 26% and 46%, respectively.

3.5. *Genotype-phenotype correlation study*

We tested the hypothesis that UGT1A1*28 is associated with erlotinib's effects on SN-38 glucuronidation activity by incubating HLMs with SN-38 in the absence or presence of erlotinib. Our previously reported genotyping analysis of this entire set of 52 Caucasian liver samples revealed 25 heterozygote (6/7) and 7 homozygote (7/7) for $(TA)_7TAA$ allele (UGT1A1*28). The remaining 20 samples were homozygote for $(TA)_6TAA$ allele (6/6, wild type).[18]

As shown in Fig. 2A, *t*-test analysis indicated that the SN-38 glucuronidation activities in the presence of erlotinib both in the whole 52 samples and among the three genotypes were significantly lower than those in the absence of erlotinib ($P < 0.01$). In addition, the SN-38 glucuronidation activities in the absence or presence of erlotinib in samples with 7/7 genotype were significantly lower than those with 6/6 ($P < 0.01$) and 6/7 genotypes ($P < 0.05$). Spearman correlation analysis revealed strong negative correlations between UGT1A1*28 in the 52 samples and SN-38G formation activity either in the absence of erlotinib ($r = -0.60$, $P < 0.0001$) or in the presence of erlotinib ($r = -0.55$, $P < 0.0001$) (Fig. 2A). No significant correlations were observed between residual activity percentage and UGT1A1*28 ($P > 0.05$) (Fig. 2B).

To investigate the influence of erlotinib concentrations on this relationship, further study was conducted in 9 liver samples (3 in each UGT1A1*28 genotype 6/6, 6/7 and 7/7). The samples were randomly selected from the samples whose volume was sufficient for further experiments. As shown in Fig. 3A–D, the SN-38 glucuronidation activities in the presence of 0, 0.15, 0.5 or 2 μM erlotinib in samples with 7/7 genotype were significantly lower than those with other genotypes (6/6 and 6/7) ($P < 0.05$). UGT1A1*28 was associated with SN-38G formation in the presence of 0, 0.15, 0.5 or 2 μM erlotinib in nine samples (Spearman $r = -0.95$, $P < 0.0005$; $r = -0.98$, $P < 0.0005$; $r = -0.90$, $P < 0.001$; $r = -0.95$, $P < 0.0005$, respectively) (Fig. 3A–D). No significant correlations were observed between the residual activity percentage and UGT1A1*28 in the same set of samples.

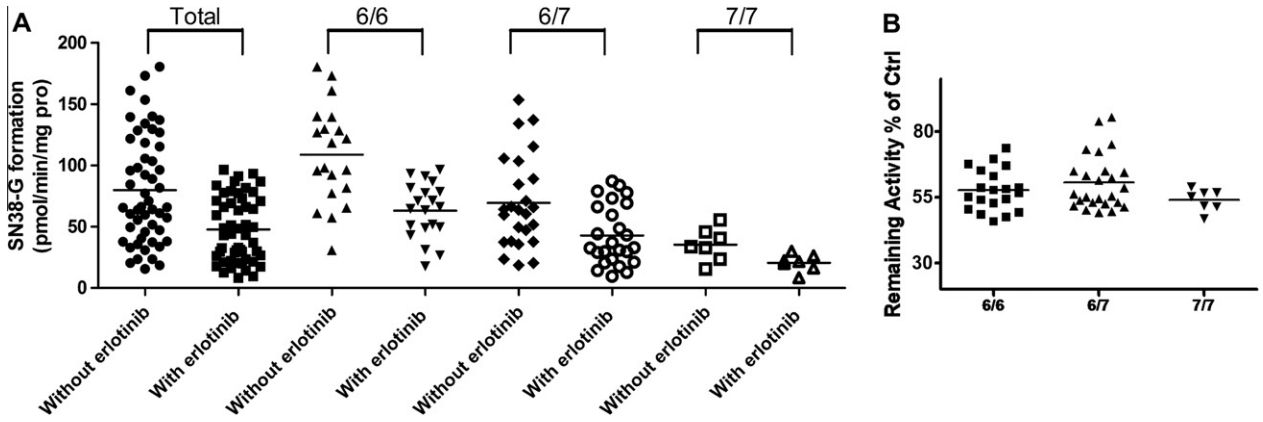

Fig. 2 – The variance in SN-38 glucuronide formation in the absence or presence of 0.5 μM erlotinib in the whole 52 Caucasian liver microsomes and among different UGT1A1*28 genotypes (A), as well as inhibition potential of erlotinib (B) in 52 Caucasian liver microsomes. Incubations were performed as described under Section 2. Data represent means of duplicate determinations.

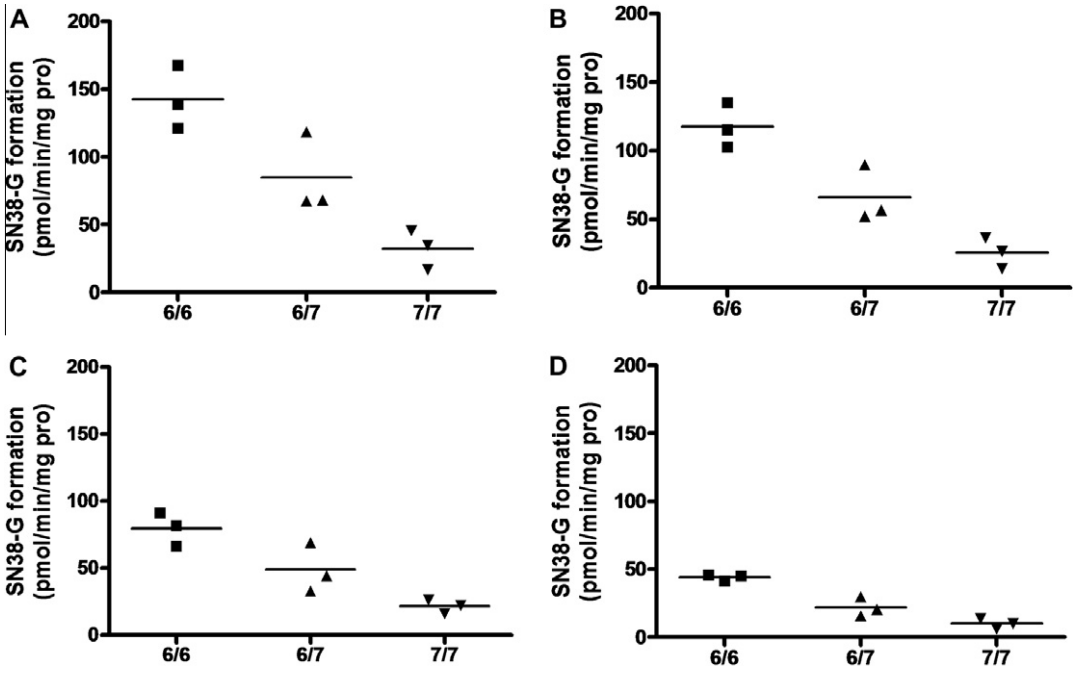

Fig. 3 – Correlation of UGT1A1*28 genotype with SN-38 glucuronide formation rates in the presence of 0 (A), 0.15 (B), 0.5 (C) or 2 μM erlotinib (D) on SN-38 glucuronidation in 9 Caucasian liver microsomes. Incubations were performed as described under Section 2. Data represent means of duplicate determinations.

4. Discussion

We demonstrated that erlotinib exhibited a UDPGA- and concentration-dependent potent inhibition against SN-38 glucuronidation activity. The inhibition type was non-competitive. This occurs when the inhibitor binds at a site away from the substrate binding site, causing a reduction in the catalytic rate. The fractional inhibition is identical at all substrate concentrations and cannot be overcome by increasing substrate concentration due to the reduction in V_{max}.[19] There are several non-competitive inhibitors of UGT enzymes that have been reported, such as phenylbutazone and quinine, which may suggest distinct binding sites for substrate and inhibitor in these enzymes.[22,23] Nevertheless, the molecular basis of these UGTs non-competitive inhibitions was unknown.

The quantitative prediction of DDI risk indicated that the coadministration of erlotinib at clinically available dose could significantly increase the AUC of SN-38, the active metabolite of irinotecan, implying that a clinically significant interaction might occur between erlotinib and irinotecan.

It is noteworthy that *in vitro* data tend to underestimate inhibition of drug glucuronidation *in vivo*,[22] and our calculation is based only on hepatic SN-38 glucuronidation, whereas the extent of extrahepatic glucuronidation is unknown. In addition, the bioavailability of erlotinib can be increased to almost 100% with the intake of food.[24] Furthermore, CYP3A4 is

involved in the metabolism of both erlotinib and irinotecan, and both irinotecan and SN-38 have been suggested to be mechanism-based inactivators of CYP3A4, making their interactions *in vivo* more complex.[25,26]

High intraluminal levels of SN-38 are believed to be the direct cause of the severe diarrhoea occurring after irinotecan therapy and high plasma levels of SN-38 are associated with neutropaenia.[2,5] Glucuronidation of SN-38 to the inactive SN-38G decreases the toxicities of irinotecan.[27] Therefore, our results may explain the unexpectedly severe toxicities found in clinical trials of the combinations of irinotecan with erlotinib.

Erlotinib also exhibited potent non-competitive inhibition against SN-38 glucuronidation in recombinant UGT1A1 with a K_i similar to that in HLMs. In view of the fact that UGT1A1, 1A3, 1A6 and 1A9 are involved in SN-38 glucuronidation and UGT1A1 shows the highest activity,[4] the inhibition of erlotinib against SN-38G formation should be attributed to the predominant inhibitory effect of erlotinib on UGT1A1 activity.

Significant correlations were observed between SN-38G formation rates in the presence of erlotinib and UGT1A1*28. Due to limitation of samples, only one concentration of erlotinib was evaluated in the whole set of human liver samples, but more detailed evaluation of nine samples in the presence of various concentrations of erlotinib lent further support to this finding. This suggests that adverse effects of the combination of irinotecan with erlotinib would be associated with the UGT1A1*28 polymorphism.

The present findings shed light on the development and optimisation of the combinations involving irinotecan and erlotinib and also provide the basis for further clinical studies investigating adverse effects of the combination of irinotecan with erlotinib.

Conflict of interest statement

Dr. Mark J. Ratain has previously served as a consultant for Ambit, Hoffman-LaRoche, OSI Pharmaceuticals and Genentech.

Acknowledgements

This work was supported by Pharmacogenetics of Anticancer Agents Research Group, National Institutes of Health (NIH)/ National Institute of General Medical Sciences Grant U01GM61393.

REFERENCES

1. Fuchs CS, Moore MR, Harker G, et al. Phase III comparison of two irinotecan dosing regimens in second-line therapy of metastatic colorectal cancer. *J Clin Oncol* 2003;**21**:807–14.
2. Innocenti F, Undevia SD, Iyer L, et al. Genetic variants in the UDP-glucuronosyltransferase 1A1 gene predict the risk of severe neutropenia of irinotecan. *J Clin Oncol* 2004;**22**:1382–8.
3. Hoskins JM, Goldberg RM, Qu P, Ibrahim JG, McLeod HL. UGT1A1*28 genotype and irinotecan-induced neutropenia: dose matters. *J Natl Cancer Inst* 2007;**99**:1290–5.
4. Hanioka N, Ozawa S, Jinno H, et al. Human liver UDP-glucuronosyltransferase isoforms involved in the glucuronidation of 7-ethyl-10-hydroxycamptothecin. *Xenobiotica* 2001;**31**:687–99.
5. Ramchandani RP, Wang Y, Booth BP, et al. The role of SN-38 exposure, UGT1A1*28 polymorphism, and baseline bilirubin level in predicting severe irinotecan toxicity. *J Clin Pharmacol* 2007;**47**:78–86.
6. Iyer L, Hall D, Das S, et al. Phenotype-genotype correlation of in vitro SN-38 (active metabolite of irinotecan) and bilirubin glucuronidation in human liver tissue with UGT1A1 promoter polymorphism. *Clin Pharmacol Ther* 1999;**65**:576–82.
7. Ando Y, Saka H, Asai G, et al. UGT1A1 genotypes and glucuronidation of SN-38, the active metabolite of irinotecan. *Ann Oncol* 1998;**9**:845–7.
8. Iyer L, Das S, Janisch L, et al. UGT1A1*28 polymorphism as a determinant of irinotecan disposition and toxicity. *Pharmacogenomics J* 2002;**2**:43–7.
9. Liu Y, Ramirez J, House L, Ratain MJ. Comparison of the drug–drug interactions potential of erlotinib and gefitinib via inhibition of UDP-glucuronosyltransferases. *Drug Metab Dispos* 2010;**38**:32–9.
10. Vokes EE, Chu E. Anti-EGFR therapies: clinical experience in colorectal, lung, and head and neck cancers. *Oncology (Williston Park)* 2006;**20**(Suppl. 2):15–25.
11. Cunningham D, Humblet Y, Siena S, et al. Cetuximab monotherapy and cetuximab plus irinotecan in irinotecan-refractory metastatic colorectal cancer. *New Engl J Med* 2004;**351**:337–45.
12. Arora A, Scholar EM. Role of tyrosine kinase inhibitors in cancer therapy. *J Pharmacol Exp Ther* 2005;**315**:971–9.
13. Chen J, Smith M, Kolinsky K, et al. Antitumor activity of HER1/EGFR tyrosine kinase inhibitor erlotinib, alone and in combination with CPT-11 (irinotecan) in human colorectal cancer xenograft models. *Cancer Chemother Pharmacol* 2007;**59**:651–9.
14. Bajetta E, Di Bartolomeo M, Buzzoni R, et al. Dose finding study of erlotinib combined to capecitabine and irinotecan in pretreated advanced colorectal cancer patients. *Cancer Chemother Pharmacol* 2009;**64**:67–72.
15. Messersmith WA, Laheru DA, Senzer NN, et al. Phase I trial of irinotecan, infusional 5-fluorouracil, and leucovorin (FOLFIRI) with erlotinib (OSI-774): early termination due to increased toxicities. *Clin Cancer Res* 2004;**10**:6522–7.
16. Iyer L, Hall D, Das S, et al. Phenotype-genotype correlation of in vitro SN-38 (active metabolite of irinotecan) and bilirubin glucuronidation in human liver tissue with UGT1A1 promoter polymorphism. *Clin Pharmacol Ther* 1999;**65**:576–82.
17. Yong WP, Ramirez J, Innocenti F, Ratain MJ. Effects of ketoconazole on glucuronidation by UDP-glucuronosyltransferase enzymes. *Clin Cancer Res* 2005;**11**:6699–704.
18. Innocenti F, Liu W, Chen P, et al. Haplotypes of variants in the UDP-glucuronosyltransferase 1A9 and 1A1 genes. *Pharmacogenet Genomics* 2005;**15**:295–301.
19. Copeland RA. *Enzymes: a practical introduction to structure, mechanism, and data analysis*. New York: Wiley-VCH; 2000.
20. Frohna P, Lu J, Eppler S, et al. Evaluation of the absolute oral bioavailability and bioequivalence of erlotinib, an inhibitor of the epidermal growth factor receptor tyrosine kinase, in a randomized, crossover study in healthy subjects. *J Clin Pharmacol* 2006;**46**:282–90.
21. Yamamoto N, Horiike A, Fujisaka Y, et al. Phase I dose-finding and pharmacokinetic study of the oral epidermal growth factor receptor tyrosine kinase inhibitor Ro50-8231 (erlotinib) in Japanese patients with solid tumors. *Cancer Chemother Pharmacol* 2008;**61**:489–96.

22. Uchaipichat V, Mackenzie PI, Elliot DJ, Miners JO. Selectivity of substrate (trifluoperazine) and inhibitor (amitriptyline, androsterone, canrenoic acid, hecogenin, phenylbutazone, quinidine, quinine, and sulfinpyrazone) "probes" for human UDP-glucuronosyltransferases. *Drug Metab Dispos* 2006;**34**:449–56.
23. Luukkanen L, Taskinen J, Kurkela M, et al. Kinetic characterization of the 1A subfamily of recombinant human UDP-glucuronosyltransferases. *Drug Metab Dispos* 2005;**33**:1017–26.
24. Smith J. Erlotinib: small-molecule targeted therapy in the treatment of non-small-cell lung cancer. *Clin Ther* 2005;**27**:1513–34.
25. Li J, Zhao M, He P, Hidalgo M, Baker SD. Differential metabolism of gefitinib and erlotinib by human cytochrome P450 enzymes. *Clin Cancer Res* 2007;**13**:3731–7.
26. Hanioka N, Ozawa S, Jinno H, et al. Interaction of irinotecan (CPT-11) and its active metabolite 7-ethyl-10-hydroxycamptothecin (SN-38) with human cytochrome P450 enzymes. *Drug Metab Dispos* 2002;**30**:391–6.
27. Gupta E, Lestingi TM, Mick R, et al. Metabolic fate of irinotecan in humans: correlation of glucuronidation with diarrhea. *Cancer Res* 1994;**54**:3723–5.